

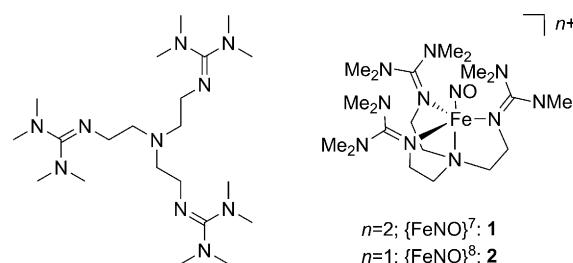
# Characterization of a High-Spin Non-Heme {FeNO}<sup>8</sup> Complex: Implications for the Reactivity of Iron Nitroxyl Species in Biology\*\*

Amy L. Speelman and Nicolai Lehnert\*

Nitric oxide (NO<sup>•</sup>) has long been implicated in numerous signaling and immune defense pathways in mammalian systems. More recently, its one-electron-reduced and potentially protonated form nitroxyl (NO<sup>−</sup>/HNO) has been shown to elicit a variety of biological responses, although the endogenous production of nitroxyl has not yet been established.<sup>[1]</sup> HNO has been suggested to bind to both ferric and ferrous hemes to yield {FeNO}<sup>7</sup>-type species (in the Enemark–Feltham notation<sup>[2]</sup>) in the former case and {Fe(H)NO}<sup>8</sup>-type species in the latter.<sup>[3]</sup> Non-heme iron centers are an alternative target for HNO, but non-heme iron nitroxyl adducts have not been well investigated. However, since non-heme {FeNO}<sup>7</sup> complexes have more positive reduction potentials than their heme counterparts, it is feasible that {FeNO}<sup>8</sup> species could be formed from non-heme {FeNO}<sup>7</sup> complexes under physiological conditions. Furthermore, non-heme {Fe(H)NO}<sup>8</sup>-type species have also been proposed as key intermediates in the catalytic cycles of bacterial respiratory NO reductases (NorBC) and flavodiiron NO reductases (FNORs).<sup>[4,5]</sup> Although multiple *low-spin* (diamagnetic) {FeNO}<sup>8</sup> model complexes have been reported previously,<sup>[6–8]</sup> there are no corresponding examples of model complexes for biological non-heme iron centers.

Herein, we report the isolation and characterization of the model complex [Fe(TMGG<sub>3</sub>tren)(NO)](OTf)<sub>2</sub> (**1**, Scheme 1), which is the first five-coordinate high-spin {FeNO}<sup>7</sup> complex with neutral N-donor ligands, and its one-electron-reduced form **2**, which is the first example of a stable high-spin {FeNO}<sup>8</sup> model complex. The spectroscopic and electronic properties of **2** are then contrasted with those of low-spin {FeNO}<sup>8</sup> species. Finally, the biological implications of the electronic structure of high-spin {FeNO}<sup>8</sup> species are discussed.

The addition of excess NO gas to a colorless solution of [Fe(TMGG<sub>3</sub>tren)(CH<sub>3</sub>CN)](OTf)<sub>2</sub> in CH<sub>3</sub>CN causes an immediate color change to black, which is indicative of the formation of **1**. NO binding leads to the appearance of an intense absorption band at 368 nm and two lower-intensity



**Scheme 1.** Structures of the ligand TMGG<sub>3</sub>tren, the model complex [Fe(TMGG<sub>3</sub>tren)(NO)](OTf)<sub>2</sub> (**1**), and the one-electron-reduced form **2**. OTf = trifluoromethanesulfonate (triflate).

features at 569 and 800 nm in the UV/Vis spectrum (Figure 1). Complex **1** has the expected high-spin ground state, as indicated by its EPR spectrum, which exhibits a rhombic

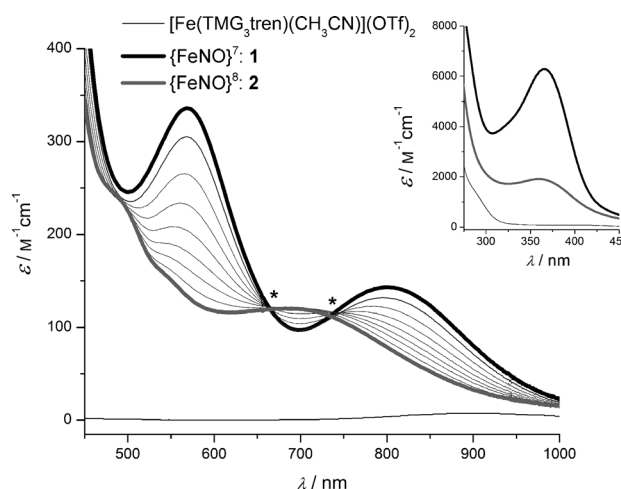


**Figure 1.** UV/Vis absorption spectra of [Fe(TMGG<sub>3</sub>tren)(CH<sub>3</sub>CN)](OTf)<sub>2</sub> and **1** in CH<sub>3</sub>CN, and of the bulk electrolysis of **1** (ca. 2 mM) to **2** in 0.1 M NBu<sub>4</sub>ClO<sub>4</sub> in CH<sub>3</sub>CN at −1.0 V versus Ag wire (transition from black to gray via thin lines). Inset: Spectra at a concentration of approximately 100 μM.

*S* = 3/2 signal (Figure 2). The FTIR spectrum of solid **1** shows an intense ν(N–O) stretching band at 1730 cm<sup>−1</sup> (see Figure S1 in the Supporting Information). The identity of **1** was further confirmed by X-ray crystallography (Figure 3).<sup>[9]</sup> As has been observed for other iron–TMGG<sub>3</sub>tren complexes, **1** has a completely trigonal bipyramidal geometry (*τ* = 1.03).<sup>[10,11]</sup> The Fe–N(O) and N–O bond lengths are typical for {FeNO}<sup>7</sup> species.<sup>[4]</sup> The Fe–N–O unit has a relatively large angle of 168°,

[\*] A. L. Speelman, Dr. N. Lehnert

Department of Chemistry, University of Michigan  
930 North University Avenue, Ann Arbor, MI 48109 (USA)  
E-mail: lehnertn@umich.edu

[\*\*] This research was supported by the National Science Foundation (CHE-1305777). A.L.S. acknowledges support from an NSF Graduate Research Fellowship (DGE-0718132). We acknowledge Dr. Jeff Kampf (University of Michigan) for the X-ray crystallographic analysis of **1** and the National Science Foundation for instrumentation (CHE-0840456).

Supporting information for this article is available on the WWW under <http://dx.doi.org/10.1002/anie.201305291>.

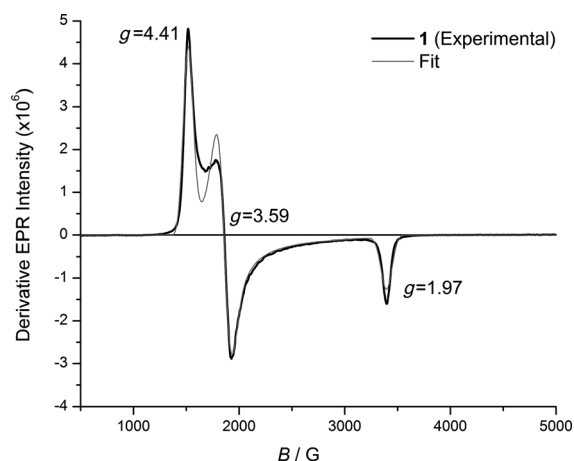


**Figure 2.** X-band EPR spectrum (shown with fit) of a frozen solution of **1** in  $\text{CH}_2\text{Cl}_2$ . Fit parameters:  $g_x = g_y = 2.01$ ,  $g_z = 2.00$ ,  $E/D = 0.070$ .

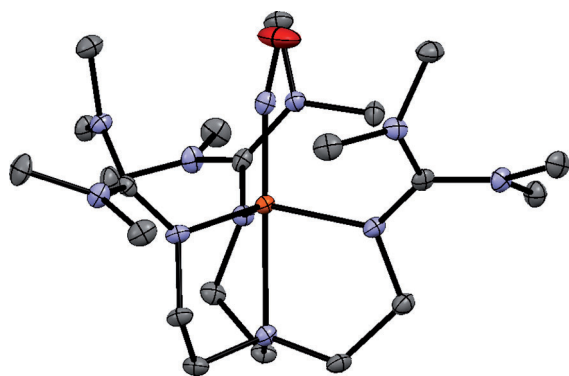


**Figure 3.** Crystal structure of **1** with ellipsoids shown at 50% probability.<sup>[9]</sup> Hydrogen atoms, counterions, and solvent molecules have been omitted for clarity. Fe orange, C gray, N blue, O red. Selected bond distances [Å] and angles [°]: Fe–N(O) 1.748, N–O 1.154, avg. Fe–N<sub>guan</sub> 2.037, Fe–N<sub>amine</sub> 2.251; Fe–N–O 168.0.

which is a result of the sterically encumbering  $\text{TMG}_3\text{tren}$  ligand.<sup>[12]</sup>

The electrochemical reduction of high-spin non-heme  $\{\text{FeNO}\}^7$  species has been reported for only a few complexes.<sup>[12–15]</sup> Importantly, the cyclic voltammograms of these complexes show quasi-reversible or irreversible  $\{\text{FeNO}\}^{7/8}$  redox couples, which suggests that the reduced species is highly unstable and hence cannot be isolated for further studies. In contrast, the cyclic voltammogram of **1** exhibits a nearly reversible redox event assigned to the  $\{\text{FeNO}\}^{7/8}$  couple at  $-1.34$  V versus  $\text{Fc}/\text{Fc}^+$  (Figure 4). The nature of this reduction was first confirmed by IR spectroelectrochemistry (Figure 5; see also Figures S2 and S3). The reduction of **1** to **2** in a thin-layer electrochemical cell is accompanied by the disappearance of the  $\nu(\text{N–O})$  stretch at  $1748\text{ cm}^{-1}$  and a splitting of the ligand guanidinium stretches at 1548 and  $1538\text{ cm}^{-1}$ .<sup>[16]</sup> Concomitantly, a new broad shoulder that overlaps with ligand bands appears at  $1618\text{ cm}^{-1}$ . This feature could be unambiguously assigned as the  $\nu(\text{N–O})$  stretch of the  $\{\text{FeNO}\}^8$  complex by comparison with the  $^{15}\text{NO}$  isotopomer.

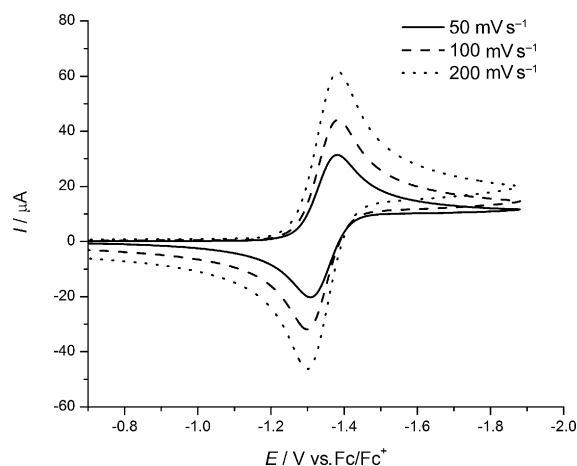


**Figure 4.** Cyclic voltammogram of **1** in a 0.1 M solution of  $\text{NBu}_4\text{ClO}_4$  in  $\text{CH}_3\text{CN}$ .  $\text{Fc}$  = ferrocene.

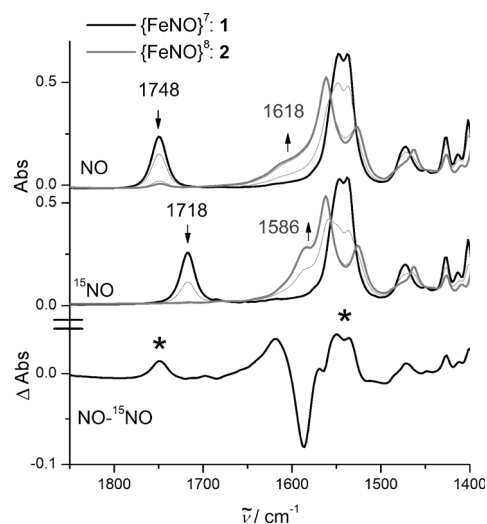


**Figure 5.** IR spectroelectrochemical analysis of the reduction of **1**-NO to **2**-NO (top) and the reduction of **1**- $^{15}\text{NO}$  to **2**- $^{15}\text{NO}$  (middle). Bottom: A difference spectrum generated by subtracting the spectrum for **2**- $^{15}\text{NO}$  from the spectrum for **2**-NO. \* denotes contributions from residual **1**-NO.

Interestingly, the  $130\text{ cm}^{-1}$  downshift in  $\nu(\text{N–O})$  upon one-electron reduction is significantly smaller than that observed in most low-spin systems (see below).

Bulk electrolysis of **1** produces a species for which the  $\nu(\text{N–O})$  band observed by solution IR spectroscopy is identical to that observed in the electrochemical cell (see Figure S4). The reduction leads to a color change from brown to yellow corresponding to a decrease in the intensity of the absorption feature at  $365\text{ nm}$  and the appearance of two new bands at  $500$  and  $700\text{ nm}$  in the UV/Vis spectrum (Figure 1). This reduction is a single, clean transformation, as indicated by the isosbestic points at  $660$  and  $750\text{ nm}$ .

To facilitate the isolation and further study of **2**, we also used chemical reductants. The treatment of **1** with equimolar  $[\text{CoCp}^*]_2$  produces **2** cleanly, as indicated by solution IR, EPR, and  $^1\text{H}$  NMR spectroscopic measurements (see Figur-

es S6, S7, and S9; Cp\* = pentamethylcyclopentadienyl). Because the [CoCp\*<sub>2</sub>]OTf by-product produced in the reaction is diamagnetic, the spin of **2** may be readily determined by <sup>1</sup>H NMR spectroscopy using the Evans method. Consistent with its  $S = 3/2$  spin state, the <sup>1</sup>H NMR spectrum of **1** exhibits multiple broad, paramagnetically shifted residues between 0 and 200 ppm (see Figure S8) and a magnetic moment of 3.9  $\mu_B$ , as measured by the Evans method. In contrast to low-spin {FeNO}<sup>8</sup> species, which are diamagnetic, **2** also shows paramagnetically shifted residues between -15 and 110 ppm (see Figure S9) and a magnetic moment of 3.1  $\mu_B$ , which is relatively close to the spin-only value for an  $S = 1$  system ( $\mu_{\text{eff}} = 2.87 \mu_B$ ). Taken together, these results demonstrate the formation of the first high-spin {FeNO}<sup>8</sup> model complex reported to date.

We used DFT calculations to further gain an understanding of the changes in bonding that occur upon reduction. The electronic structure of **1** is consistent with the previously proposed bonding description for high-spin {FeNO}<sup>7</sup> complexes, according to which high-spin Fe<sup>III</sup> is antiferromagnetically coupled to a triplet NO<sup>-</sup> ( $S = 1$ ).<sup>[4,13,17]</sup> Correspondingly, in the  $\alpha$ -spin manifold, the empty NO  $\pi^*$  orbitals form a weak  $\pi$  back bond with the occupied iron d<sub>xz</sub> and d<sub>yz</sub> orbitals (in a coordinate system in which the  $z$  axis corresponds to the Fe–N(O) bond). In the  $\beta$ -spin manifold, the occupied NO  $\pi^*$  orbitals donate strongly into the unoccupied iron d<sub>xz</sub> and d<sub>yz</sub> orbitals (Figure 6, left). The important question is how the

electronic structure changes upon reduction, and where the additional electron is localized in **2**. The calculations show that the extra electron occupies the d<sub>xy</sub> orbital of iron and thus indicate that the high-spin complex **1** undergoes a *metal-centered* reduction (Figure 6, right). The increased electron density of the iron center then causes a moderate decrease in  $\pi$  donation from NO<sup>-</sup> to Fe<sup>II</sup> in the {FeNO}<sup>8</sup> complex, and this induces the observed moderate decrease in  $\nu(\text{N–O})$ . This decrease in  $\pi$  donation in **2** is directly reflected by the increased NO  $\pi^*$  character of the  $\beta$ -spin orbitals of **2** relative to **1** (see Figure 6). In summary, these results are indicative of decreased covalency in the Fe–NO unit upon one-electron reduction, and therefore a weaker Fe–NO bond.

In contrast to these findings, the reduction of low-spin {FeNO}<sup>7</sup> complexes ( $S = 1/2$ ;  $S_{\text{Fe}} = 0$ ,  $S_{\text{NO}} = 1/2$ ) has been observed to be *NO-centered* and to lead to a diamagnetic species in which the coordinated NO<sup>-</sup> ligand is in the singlet state. For example, in [Fe(cyclam-ac)(NO)] (cyclam-ac = 1,4,8,11-tetraazacyclotetradecane-1-acetate), reduction is almost entirely NO-centered, as reflected by its large  $\nu(\text{N–O})$  downshift of 336 cm<sup>-1</sup>.<sup>[8]</sup> In heme systems, DFT calculations have revealed an electronic structure of the {FeNO}<sup>8</sup> species that is intermediate between low-spin Fe<sup>II</sup>–NO<sup>-</sup> and Fe<sup>I</sup>–NO<sup>•</sup>.<sup>[6c,d,18]</sup> Thus, heme {FeNO}<sup>8</sup> complexes show somewhat reduced downshifts of about 200 cm<sup>-1</sup> in  $\nu(\text{N–O})$ ; however, these shifts are still much larger than that observed for **2** (see Table S1).

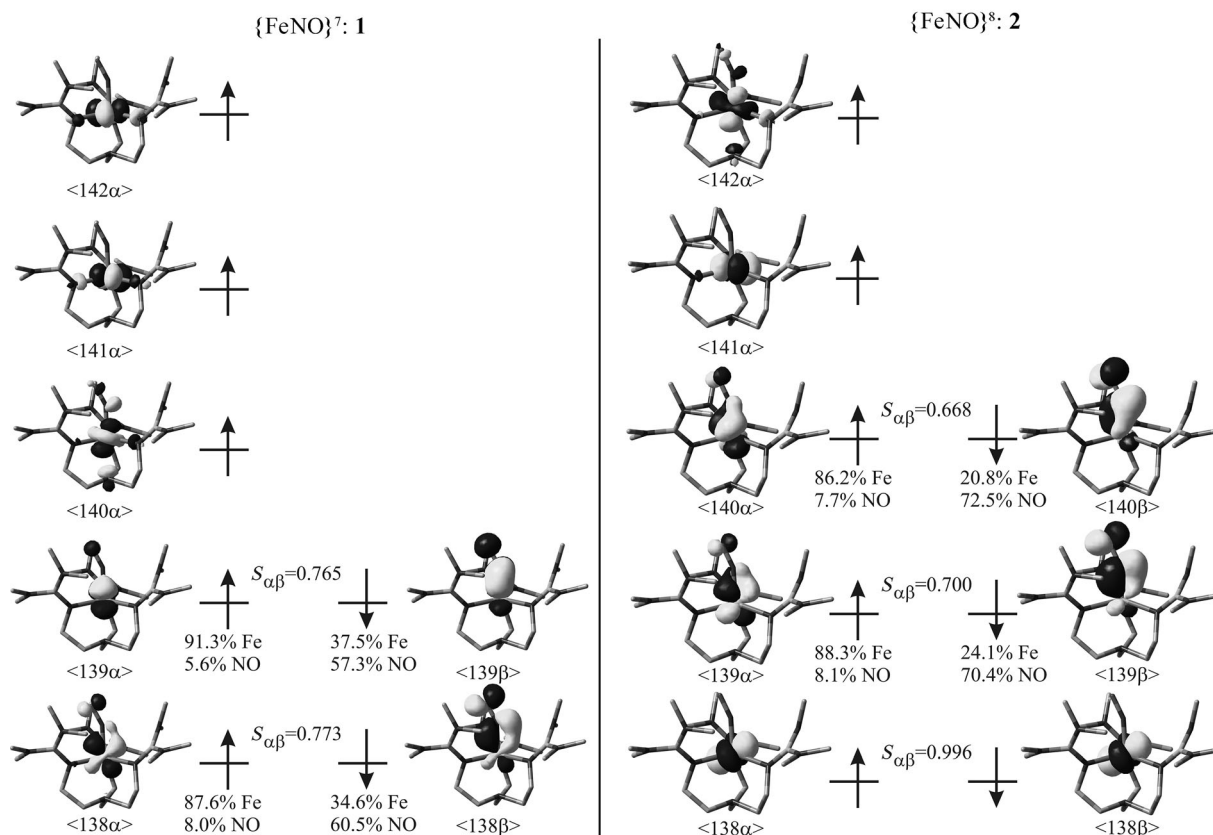


**Figure 6.** Schematic molecular-orbital diagrams of **1** (left) and **2** (right).  $S_{\alpha\beta}$  indicates the degree of spatial overlap between the  $\alpha$ - and  $\beta$ -spin orbitals.

The proposed metal-centered reduction and decreased Fe–NO covalency in high-spin non-heme {FeNO}<sup>8</sup> species as compared to {FeNO}<sup>7</sup> complexes has implications for the basicity and reactivity of non-heme iron nitroxyl complexes. Owing to the high degree of covalency of the Fe–NO bond, {FeNO}<sup>7</sup> units are generally stable and unreactive, and cannot be protonated. Correspondingly, whereas **1** shows no reactivity upon the addition of a weak acid (see Figure S10), **2** reacts immediately with the acid to form a purple species **3**, which decays within approximately 1 min at room temperature (Figure 7). Low-temperature studies of this potential

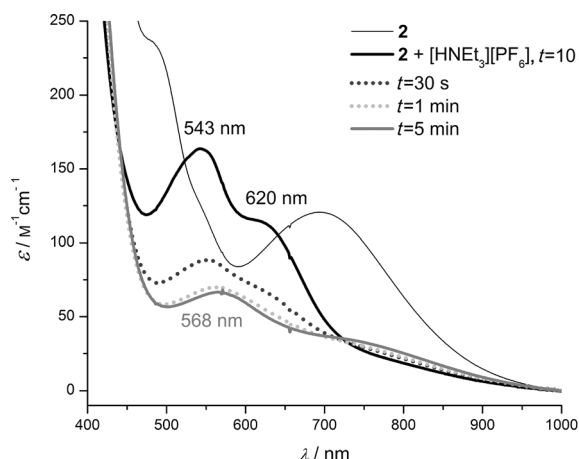


**Figure 7.** UV/Vis spectra showing the rapid decomposition of **2** upon the addition of [HNEt<sub>3</sub>][PF<sub>6</sub>] (1.2 equiv).

{Fe–HNO}<sup>8</sup> complex are currently underway. Interestingly, this result indicates that in the high-spin {FeNO}<sup>8</sup> complex **2**, the basicity of the NO<sup>−</sup> ligand is greatly increased despite the fact that the reduction is metal-centered.<sup>[19]</sup> In line with this increased basicity, heat annealing of the cryoreduced NO adduct of ferrous taurine:α-ketoglutarate dioxygenase (TauD) leads to the formation of a new species, which is proposed to be an [Fe–(H)NO]<sup>8</sup> intermediate.<sup>[20]</sup> Reduction also promotes other reactivity; for example, reduction of the stable diferrous dinitrosyl FNOR model complex [Fe<sub>2</sub>-(BPMP)(OPr)(NO)<sub>2</sub>](BPh<sub>4</sub>)<sub>2</sub> (BPMP = 2,6-bis[[bis(2-pyridylmethyl)amino]methyl]-4-methylphenolate) to the corresponding [{FeNO}<sup>8</sup>]<sub>2</sub> dimer leads to the rapid, quantitative production of N<sub>2</sub>O.<sup>[21]</sup> Overall, these results suggest that reduction serves as a potent method for the activation of stable non-heme {FeNO}<sup>7</sup> units for further reactivity.

In conclusion, we have reported herein the first example of a high-spin non-heme {FeNO}<sup>8</sup> model complex. In contrast to low-spin {FeNO}<sup>8</sup> systems, which undergo NO-centered reduction and are diamagnetic, **1** undergoes iron-centered reduction (into d<sub>xy</sub>) to an S = 1 species in which a triplet NO<sup>−</sup> ligand is bound to a high-spin ferrous center. Interestingly, a similar electronic structure was proposed for the {FeNO}<sup>8</sup> adduct of TauD;<sup>[20]</sup> thus, metal-centered reduction may be a general feature of high-spin {FeNO}<sup>7/8</sup> systems. Because the ligand TMG<sub>3</sub>tren is an extremely strong donor, the reduction of **1** occurs at a relatively negative potential. However,

biological donors are much weaker ligands; therefore, biological non-heme iron nitrosyl complexes are expected to undergo reduction at more positive, biologically feasible potentials. Accordingly, the non-heme {FeNO}<sup>7</sup> model complexes [Fe(BMPA-Pr)(NO)]X (X = ClO<sub>4</sub><sup>−</sup>, OTf<sup>−</sup>; BMPA-Pr = N-propanoate-N,N-bis(2-pyridylmethyl)amine) undergo reduction at approximately −300 mV versus the normal hydrogen electrode (NHE).<sup>[13]</sup> This result suggests that non-heme iron centers could potentially function as HNO synthases in vivo, if HNO loss from these complexes was facile. Importantly, the decreased covalency in the Fe–NO unit that results from the reduction makes high-spin {FeNO}<sup>8</sup> complexes reactive towards weak acids and amenable to other chemical transformations. In particular, {FeNO}<sup>8</sup> species could be central intermediates responsible for the key N–N bond forming step in NO reductases.<sup>[4]</sup>

Received: June 19, 2013

Revised: August 22, 2013

Published online: October 2, 2013

**Keywords:** bioinorganic chemistry · nitrogen oxides · nitroxyl complexes · non-heme iron · reduction

- [1] K. M. Miranda, *Coord. Chem. Rev.* **2005**, *249*, 433–455.
- [2] J. H. Enemark, R. D. Feltham, *Coord. Chem. Rev.* **1974**, *13*, 339–406.
- [3] R. Lin, P. J. Farmer, *J. Am. Chem. Soc.* **2000**, *122*, 2393–2394.
- [4] T. C. Berto, A. L. Speelman, S. Zheng, N. Lehnert, *Coord. Chem. Rev.* **2013**, *257*, 244–259.
- [5] J. D. M. Kurtz, Jr., *Dalton Trans.* **2007**, 4115–4121.
- [6] a) D. Lancon, K. M. Kadish, *J. Am. Chem. Soc.* **1983**, *105*, 5610–5617; b) I. K. Choi, Y. Liu, D. Feng, K. J. Paeng, M. D. Ryan, *Inorg. Chem.* **1991**, *30*, 1832–1839; c) J. Pellegrino, S. E. Bari, D. E. Bikiel, F. Doctorovich, *J. Am. Chem. Soc.* **2010**, *132*, 989–995; d) L. E. Goodrich, S. Roy, E. E. Alp, J. Zhao, M. Y. Hu, N. Lehnert, *Inorg. Chem.* **2013**, *52*, 7766–7780.
- [7] A. K. Patra, K. S. Dube, B. C. Sanders, G. C. Papaefthymiou, J. Conradie, A. Ghosh, T. C. Harrop, *Chem. Sci.* **2012**, *3*, 364–369.
- [8] R. García-Serres, C. A. Grapperhaus, E. Bothe, E. Bill, T. Weyhermüller, F. Neese, K. Wieghardt, *J. Am. Chem. Soc.* **2004**, *126*, 5138–5153.
- [9] Experimental details for the acquisition of crystal data and structure refinement can be found in the Supporting Information. CCDC 945365 contains the supplementary crystallographic data for this paper. These data can be obtained free of charge from The Cambridge Crystallographic Data Centre via [www.ccdc.cam.ac.uk/data\\_request/cif](http://www.ccdc.cam.ac.uk/data_request/cif).
- [10] a) J. England, E. R. Farquhar, Y. Guo, M. A. Cranswick, K. Ray, E. Münck, L. Que, *Inorg. Chem.* **2011**, *50*, 2885–2896; b) J. England, Y. Guo, E. R. Farquhar, V. G. Young, Jr., E. Münck, L. Que, Jr., *J. Am. Chem. Soc.* **2010**, *132*, 8635–8644; c) H. Wittmann, V. Raab, A. Schorm, J. Plackmeyer, J. Sundermeyer, *Eur. J. Inorg. Chem.* **2001**, 1937–1948.
- [11] As noted previously,<sup>[10a]</sup> the large  $\tau$  value (> 1) presumably arises from the 0.364 Å displacement of the Fe center from the mean plane defined by the equatorial nitrogen atoms.
- [12] M. Ray, A. P. Golombek, M. P. Hendrich, G. P. A. Yap, L. M. Liable-Sands, A. L. Rheingold, A. S. Borovik, *Inorg. Chem.* **1999**, *38*, 3110–3115.
- [13] T. C. Berto, M. B. Hoffman, Y. Murata, K. B. Landenberger, E. E. Alp, J. Zhao, N. Lehnert, *J. Am. Chem. Soc.* **2011**, *133*, 16714–16717.

- [14] K. Pohl, K. Wieghardt, B. Nuber, J. Weiss, *J. Chem. Soc. Dalton Trans.* **1987**, 187–192.
- [15] Z. J. Tonzetich, F. Héroguel, L. H. Do, S. J. Lippard, *Inorg. Chem.* **2011**, 50, 1570–1579.
- [16] The parent complex  $[\text{Fe}(\text{TMG}_3\text{tren})(\text{CH}_3\text{CN})]^{2+}$  shows only an irreversible reductive event at approximately  $-2.5\text{ V}$  versus ferrocene,<sup>[10c]</sup> which indicates that the reduction of **1** is not ligand-based. This conclusion is supported by DFT calculations, which show only a small change in spin density on the ligand in **2** as compared to **1** (see Table S3 in the Supporting Information). Rather, the splitting in the ligand bands is indicative of changes in the covalency of the iron–TMG<sub>3</sub>tren unit.
- [17] C. A. Brown, M. A. Pavlosky, T. E. Westre, Y. Zhang, B. Hedman, K. O. Hodgson, E. I. Solomon, *J. Am. Chem. Soc.* **1995**, 117, 715–732.
- [18] N. Lehnert, V. K. K. Praneeth, F. Paulat, *J. Comput. Chem.* **2006**, 27, 1338–1351.
- [19] No experimental  $\text{p}K_{\text{a}}$  values for biological  $\{\text{FeHNO}\}^8$ -type complexes have been reported; however, DFT calculations suggest that **2** is less basic than the corresponding low-spin (heme) complexes (see the Supporting Information).
- [20] S. Ye, J. C. Price, E. W. Barr, M. T. Green, J. M. Bollinger, C. Krebs, F. Neese, *J. Am. Chem. Soc.* **2010**, 132, 4739–4751.
- [21] S. Zheng, T. C. Berto, E. W. Dahl, M. B. Hoffman, A. L. Speelman, N. Lehnert, *J. Am. Chem. Soc.* **2013**, 135, 4902–4905.